HHS Public Access

Author manuscript

Clin Genet. Author manuscript; available in PMC 2021 February 01.

Published in final edited form as:

Clin Genet. 2020 February ; 97(2): 338–346. doi:10.1111/cge.13665.

Phenotype-to-genotype approach reveals head-circumference-associated genes in an autism spectrum disorder cohort

Huidan Wu[1], **Honghui Li**[2], **Ting Bai**[1], **Lin Han**[1], **Jianjun Ou**[3], **Guanglei Xun**[4], **Yu Zhang**[2], **Yazhe Wang**[5], **Guiqin Duan**[5], **Ningxia Zhao**[6], **Biyuan Chen**[7], **Xiaogang Du**[6], **Meiling Yao**[5], **Xiaobing Zou**[7], **Jingping Zhao**[3], **Zhengmao Hu**[1], **Evan E. Eichler**[9,10], **Hui Guo**[1,9,11], **Kun Xia**[1,12,13]

[1]Center for Medical Genetics & Hunan Provincial Key Laboratory of Medical Genetics, School of Life Sciences, Central South University, Changsha, Hunan, China.

[2]Key Laboratory of Developmental Disorders in Children, Liuzhou Maternity and Child Healthcare Hospital, Liuzhou, Guangxi, China.

[3]Mental Health Institute of the Second Xiangya Hospital, Central South University, Changsha, Hunan, China.

[4]Mental Health Center of Shandong Province, Jinan, Shandong, China.

[5]Center of Children Psychology and Behavior, Third Affiliated Hospital of Zhengzhou University, Zhengzhou, Henan China.

[6]Xi'an Encephalopathy Hospital of Traditional Chinese Medicine, Xi'an, Shanxi, China.

[7]Children Development Behavior Center of the Third Affiliated Hospital of SUN YAT-SEN University, Guangzhou, Guangdong, China.

[9]Department of Genome Sciences, University of Washington School of Medicine, Seattle, Washington, USA.

[10]Howard Hughes Medical Institute, University of Washington, Seattle, Washington, USA.

[11]Hunan Key Laboratory of Animal Models for Human Diseases, Changsha 410078, China.

[12]Key Laboratory of Medical Information Research, Central South University, Changsha, Hunan, China.

[13]Collaborative Innovation Center for Genetics and Development, Shanghai, China.

Abstract

The genotype-first approach has been successfully applied and has elucidated several subtypes of autism spectrum disorder (ASD). However, it requires very large cohorts because of the extensive genetic heterogeneity. We investigate the alternate possibility of whether phenotype-specific genes

Correspondence: Hui Guo (guohui@sklmg.edu.cn) or Kun Xia (xiakun@sklmg.edu.cn).

Competing interests

E.E.E. is on the scientific advisory board (SAB) of DNAnexus, Inc. All other authors declare no competing financial interests.

All data needed to evaluate the conclusions in the paper are present in the paper and/or the Supplementary Materials. Additional data related to this paper may be requested from the authors.

can be identified from a small group of patients with specific phenotype(s). To identify novel genes associated with ASD and abnormal head circumference using a phenotype-to-genotype approach, we performed whole-exome sequencing on 67 families with ASD and abnormal head circumference. Clinically relevant pathogenic or likely pathogenic variants account for 23.9% of patients with microcephaly or macrocephaly, and 81.25% of those variants or genes are head-size associated. Significantly, recurrent pathogenic mutations were identified in two macrocephaly genes (*PTEN*, *CHD8*) in this small cohort. *De novo* mutations in several candidate genes (*UBN2*, *BIRC6*, *SYNE1*, and *KCNMA1*) were detected, as well as one new candidate gene (*TNPO3*,) implicated in ASD and related neurodevelopmental disorders. We identify genotype–phenotype correlations for head-size-associated ASD genes and novel candidate genes for further investigation. Our results also suggest a phenotype-to-genotype strategy would accelerate the elucidation of genotype–phenotype relationships for ASD by using phenotype-restricted cohorts.

Graphical Abstract

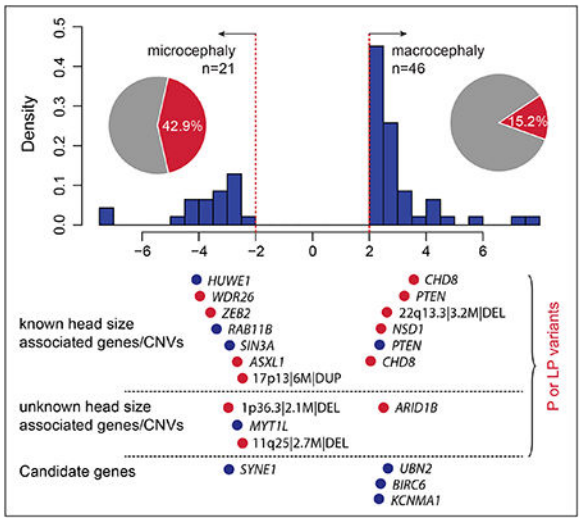

Keywords

Autism spectrum disorder; whole-exome sequencing; microcephaly; macrocephaly; genotype and phenotype correlations

Introduction

Autism spectrum disorder (ASD) is a group of phenotypic heterogeneous neurodevelopmental disorders (NDDs) with global prevalence around 1%[1]. Besides the core symptoms, a deficit in social communication and restricted and repetitive behaviors, ASD has a large group of clinical manifestations, such as language disability, intellectual disability (ID), seizure, abnormal head size, gastrointestinal (GI) problems and so on[2]. To date, *de novo* and rare gene-disruptive mutations and copy number variants (CNVs) have been found to contribute a significant proportion to the ASD genetic architecture[3]. However, because of the extremely rare variants of each gene, very large cohorts are needed to prove

the significance of an individual gene. We are in the early stages of understanding genotype–phenotype relationships for most risk genes.

ASD genotype–phenotype correlations are important to identify phenotypic subtypes and for early diagnosis and clinical management. The genotype-to-phenotype approach has elucidated several subtypes of ASD, such as *CHD8*[4], *DYRK1A*[5] and *ADNP*[6]. These studies provide evidence that patients with disruptive mutations at specific genes or CNVs are more likely to share distinctively similar phenotypes. For example, patients with truncating mutations in *CHD8* most likely present with macrocephaly, GI disturbance and general overgrowth; patient with truncated mutations in *DYRK1A*, in contrast, show microcephaly, distinctive facial features and ID. Although the genotype-first approach has been successfully applied, it requires very large cohorts because of the extensive genetic heterogeneity[7]. Here, we investigate the alternate possibility of whether phenotype-specific genes can be identified from a small group of patients with specific phenotype(s).

Abnormal head size has long been recognized as a co-occurring condition of ASD. Leo Kanner originally described macrocephaly in ASD in 1943[1]. It is estimated that about 20% of ASD patients have increased head size[8]. Mutations of several ASD genes have been reported causing macrocephaly, such as *PTEN*[9] and *CHD8*[4]. Meanwhile, microcephaly was also frequently noticed in ASD patients. For example, patients with *DYRK1A*[5] and *CDKL5*[10] truncated mutations more likely present with microcephaly. Patients with deletion and duplication of 16p11.2 have opposing head sizes. The deletion is associated with increased head size, whereas the duplication is associated with decreased head size[11]. Moreover, patients with *de novo* mutations (DNMs) within genes involved in the β-catenin/Wnt-signaling pathway, which is important in transcription regulation, present reciprocal macrocephaly and microcephaly[7].

To test the efficiency of the phenotype-to-genotype approach and identify genes associated with ASD patients and abnormal head size, we sequenced 92 ASD families with abnormal head circumference size. Clinically relevant pathogenic or likely pathogenic events were identified in 17.4% of probands, and most of them are already known to be associated with microcephaly or macrocephaly. Our study implicates new variants and genes for ASD and abnormal head size for future investigation.

Materials and Methods

Patients recruitment and ethical approval

We selected 67 ASD families (58 trios, 9 simplex quads, 210 individuals) from the Autism Clinical and Genetic Resources in China (ACGC) cohort[11] for whole-exome sequencing (WES) (Figure 1). Out of 43 trios and three simplex quads, 46 probands have macrocephaly (> +2 standard deviations (SD)); and 21 probands, from 15 trios and six simplex quads, have microcephaly (< −2SD) (Figure 1b, supplementary table S1). All probands were diagnosed according to DSM-IV or DSM-V by experienced clinicians. In addition, co-occurring conditions including medical problems, such as epilepsy, gastrointestinal issues and sleep disorders; developmental diagnoses, such as intellectual disability and language delay; and mental-health conditions, such as attention deficit hyperactivity disorder (ADHD),

obsessive-compulsive disorder and depression, were collected for presenting patients. Peripheral blood of all involved individuals was collected with informed consent. This study is in accordance with the ethical standards of the Institutional Review Board of the School of Life Sciences at Central South University, Changsha, Hunan, China.

Whole-exome sequencing and single-nucleotide variants (SNVs)/indels calling

Genomic DNA was extracted from the whole blood using a standard proteinase K digestion and the phenol-chloroform method. All samples were captured using SureSelect Human All Exon V6 Library (Agilent) reagents. The pools were then sequenced on the Illumina HiSeq X Ten platform using paired-end 150 bp reads. Clean FASTQ reads were mapped to the reference genome assembly (hg38) using BWA-MEM (v.0.6)[12]. PCR duplicates were marked using Picard (http://broadinstitute.github.io/picard/) MarkDuplicates (v.2.9.4). Bases were recalibrated using Genome Analysis Toolkit (GATK v.3.7–2) BaseRecalibrator[13]. Genotypes were then generated with GATK HaplotypeCaller (v.3.7–2) on a per-family basis.

De novo SNV/indel discovery and validation

Family relationships were assessed using the KING program[14]. *De novo* SNVs and indels were called using a custom *de novo* filtering pipeline as previously described[15]. In brief, the pipeline uses the family-level Variant Call Format (VCF) files; candidate sites were chosen where the parents genotypes are 0/0 and the children's genotypes are either 0/1 or 1/1. The allele count, read depth, and allele balance were filtered as follows: parental alternate allele count is equal to zero, child allele balance is above 0.25, read depth for all family members is above 10, and child genotype quality was above 20. Merged VCF files were annotated using ANNOVAR[16], which annotates different functions of the variants in extensively specific databases, such as population control databases (ExAC, gnomAD, 1000 Genomes Project etc.), functional prediction databases (SIFT, PolyPhen2, MutationTaster, etc.), dbSNP, etc. We applied Sanger sequencing to validate *de novo* SNVs and indels.

CNV discovery and validation

CNVs were called using XHMM algorithms according to the best-practice guidelines[17]. In brief, GATK was used to calculate depth of coverage (from BWA-MEM alignments) for each individual, and all individuals were then combined into one composite file. The XHMM-specific steps included hard filtering of samples and targets, PCA on the data, filtering based on the PCA results and discovery of CNVs. Post-discovery CNVs were genotyped by family, and a score cutoff of 10 was ultimately used to determine inheritance in families using SQ and NQ values. Quantitative PCR performed using the Roche LightCycler® 96 System (F. Hoffmann-La Roche AG, Basel, Switzerland), was used to validate the large *de novo* CNVs called by XHMM. Three pairs of primers were selected from the start, middle, and end of each CNV, separately. The sample was analyzed in triplicate in a 10μl reaction mixture. The values were evaluated using the LightCycler® 96 Application Software Version 1.1 (F. Hoffmann-La Roche AG, Basel, Switzerland). Further data analysis was performed using the qBase method.

Statistical analyses

To identify potential novel candidate genes, we leveraged DNM data from published whole-exome or whole-genome sequencing of 10,842 cases with NDDs, including 5,578 cases with a diagnosis of ASD and 5,264 cases with a diagnosis of ID/developmental delay (DD) collected from five studies[18–22] in denovo-db (v.1.5)[23]. Genes with a significant excess of DNMs from this study and the above reported studies were identified using two statistical models. The first is a probabilistic model that incorporates the overall rate of mutation in coding sequences, estimates of relative locus-specific rates based on chimpanzee–human fixed differences derived from the chimpanzee–human divergence (CH) model[24]. The second, denovolyzeR, estimates mutation rates based on trinucleotide context and accommodates known mutational biases such as CpG hotspots (denovolyzeR model)[25]. Both models are well explored for DNM analysis in multiple studies. Default parameters were used for both models. An expected rate of 1.5 DNMs per exome was used for the CH model. *P* values were corrected for genome-wide multiple testing using the Bonferroni method (n = 18,946 in CH model; n = 19,618 in denovolyzeR).

Results

Variants discovery and diagnostic yields

We sequenced the protein-coding portion for all individuals with a mean depth of 90 ± 5.3x (Figure 1c). Over 97% of the CCDS region was sequenced over ten times (Figure 1d). All family relationships were confirmed based on variant transmission analysis. We detected 121 *de novo* SNVs and indels in exomes (supplementary table S2). We attempted to validate all rare (<0.1% in ExAC) *de novo* non-synonymous SNVs/indels (n = 68). We validated 62 rare SNVs/indels as *de novo* (five SNVs were validated as false positive, and one located in the segmental duplication region was not resolved by Sanger sequencing) (supplementary table S3). three false positive variants of the five have low alternative allele depth (<5). For the inherited variants, we identified 48 inherited rare likely gene-disruptive (LGD) variants (supplementary table S4). Considering the difficulties associated with exome-based CNV analysis[26], we only considered and validated large CNVs with sizes greater than 1 Mbp. Four large CNVs were identified and successfully validated as *de novo* (supplementary figure S1).

To evaluate the WES diagnostic yield and evaluate the phenotypes corresponding to clinically relevant pathogenic or likely pathogenic variants, we classified the variants described above following the standards and guidelines for the interpretation of sequence variants and CNVs from the American College of Medical Genetics and Genomics (ACMG)[27,28]. In total, we classified 17 clinically relevant pathogenic or likely pathogenic events from 16 patients, including 13 SNVs/indels (7 *de novo* LGD, 5 *de novo* missense and 1 inherited LGD mutation) (Table 1) and 4 *de novo* CNVs (Table 2). Overall, clinically relevant pathogenic or likely pathogenic variants account for 23.9% patients (16/67). Pathogenic or likely pathogenic variants account for 42.9% patients with microcephaly (9/21, 42.9%) and 15.2% patients with macrocephaly (7/46, 15.2%) (Figure 2a, b). (Table 1, Figure 2b). The diagnostic yield (18%, 12/67) is 2-fold higher than the diagnostic yield

(8.9%) among a recent larger unselected ASD cohorts when only considering the SNV/indels[29].

Clinically relevant variants within known head-circumference-associated genes and corresponding phenotypes

Among the 17 clinically relevant pathogenic or likely pathogenic variants identified in microcephaly or macrocephaly patients, 13 of them are already known to be associated with abnormal head size, which accounts for 81.25% of this clinically resolved patient subset (Figure 2b). Five pathogenic or likely pathogenic variants within three macrocephaly-related genes (*PTEN*, *CHD8*, and *NSD1*) and one pathogenic macrocephaly-related CNV (22q13.3 deletion) were identified in six patients with macrocephaly (Table 1, Table 2). Pathogenic or likely pathogenic variants of *PTEN* (1 LGD DNM and 1 missense DNM) and *CHD8* (1 LGD DNM and 1 inherited LGD mutation) were recurrently identified in two individuals with macrocephaly respectively, and both are well-defined macrocephaly-related genes. Importantly, for the inherited *CHD8* LGD mutation (GX0540.p1, p.N885Tfs*14), the carrier father shows increased head size (1.53 SD). In addition, the carrier father also shows autistic traits with high Broad Autism Phenotype Questionnaire score across the domains of autism and NVIQ scores in the borderline range (NVIQ = 79) as we reported in our recently targeted sequencing paper[30]. *NSD1* mutations cause Sotos syndrome, a syndromic ASD with macrocephaly as a recurrent phenotype. Besides ASD and macrocephaly, our patient with the *NSD1* LGD DNM also presents with ID, language developmental delay, sleeping problems, and attention deficit hyperactivity disorder (ADHD) (supplementary table S5). Macrocephaly was recurrently reported in patients with Phelan-McDermid syndrome, which is caused by the 22q13.3 deletion. Besides ASD and macrocephaly, this patient also showed ID, motor and language development delay, sleeping problems, ADHD, and obsessive behavior, which is consistent with the phenotypes of Phelan-McDermid syndrome.

Six pathogenic or likely pathogenic variants in six microcephaly-related genes, including *ZEB2*, *ASXL1*, *WDR26*, *SIN3A*, *RAB11B* and *HUWE1*, and one pathogenic microcephaly-related CNV (17p13.2–13.3 duplication) were identified in seven patients with microcephaly (Table 1, Table 2). *ZEB2* mutations cause microcephaly-related syndromic ASD (Mowat–Wilson syndrome). Besides autistic phenotypes and microcephaly (−3.55 SD), other phenotypes, including ID, motor and language development delay, abnormal MRI and EEG, sleeping problems, and GI problems, were also present in our patient (supplementary table S5). *ASXL1* LGD mutations cause Bohring-Opitz syndrome, which is characterized by severe developmental delay and microcephaly. Loss-of-function mutations of *SIN3A* are associated with mild ID and often accompanied by ASD and microcephaly. Although the missense mutation we identified here is likely pathogenic, the phenotypes of our patient are consistent with the reported patients: ASD, ID, microcephaly (−2.77 SD), abnormal MRI, and ADHD. Dozens of missense mutations of *HUWE1* have been reported in association with ASD and other NDDs. The missense DNM in our patients is located in the HECT domain, where clustered missense mutations have been observed[31], and it is very close to the missense mutations co-segregating with the phenotype in multiple-generation families[32]. Interestingly, most of the patients (6/9) with DNMs in HECT regions present microcephaly[31]. Chromosome 17p13.3 duplication causes multiple complex NDD

phenotypes, including mild to severe developmental phenotypes, ASD, and mild brain malformations including microcephaly[2]. Our patient presents with ASD, ID, language developmental delay, abnormal MRI, and ADHD. All these phenotypes were recurrently observed in reported patients with chromosome 17p13.3 duplications. Notably, in addition to the 17p13.3 duplication, our patient also carried a 2.7 Mbp pathogenic deletion leading to loss of *NTM*, an ASD candidate gene. However, no variation in head size was previously reported for this CNV.

Mutations of *WDR26* and *RAB11B* were recently identified for broad NDD phenotypes[33,34]. Most patients with mutations within these two genes show microcephaly. In addition to ASD and microcephaly (−3.92 SD), our patient with the *WDR26* LGD DNM also presents ID, seizure, language developmental delay, abnormal MRI, sleeping problems, and ADHD, which are similar to the patients reported here (supplementary table S5). The missense mutation within *RAB11B* identified in our patient is located in the reported pathogenic missense cluster within the nucleotide-binding domain, which is important for GTP binding (Figure 3). In addition to ASD and microcephaly (−3.31 SD), the patient also presents with ID, language developmental delay, abnormal EEG and MRI, and ADHD.

De novo variants in ASD candidate genes

In addition to clinically relevant pathogenic or likely pathogenic variants, four missense DNMs within four ASD candidate genes (SFARI: https://gene.sfari.org/), including *UBN2* (p.R535C), *BIRC6* (p.T4293I), *KCNMA1* (p.R1083K) and *SYNE1* (p.R7507H), were identified in three patients with macrocephaly and one patient with microcephaly (Table 1, Figure 2). We applied the Combined Annotation Dependent Depletion (CADD) score as well as other functional prediction tools to predict the damaging effect of these missense DNMs in gene function (supplementary table S2). The missense DNM within *UBN2*, previously associated with ASD[19], has a CADD score of 35 and is predicted as damaging by both SIFT and Polyphen2 (supplementary table S2). Two LGD DNMs and three missense DNMs were reported in NDDs (Figure 3, supplementary table S6). Two LGD DNMs and one missense DNM are from ASD, and two missense DNMs are from DD. The number of DNMs among individuals with NDD is nominally significant ($P = 4.7 \times 10^{-5}$, CH model; $P = 4.5 \times 10^{-4}$, denovolyzeR model) although neither survives genome-wide multiple comparisons.

By leveraging DNMs identified from the published NDD cohorts, we identified a potential new candidate gene in ASD and related NDDs. We identified one missense DNM (p.C672S) in *TNPO3* (CADD = 22) and seven DNMs (2 LGD, 5 missense) from previously published large-scale sequencing studies (Figure 3, supplementary table S6). We calculated the probability of detecting eight or more DNMs (including LGD and missense) in the combined NDD cohorts (n = 10842) and find an excess of *TNPO3* DNMs in NDD patients ($P = 5.9 \times 10^{-8}$, $P_{adj} = 0.001$, CH model; $P = 1.3 \times 10^{-6}$, $P_{adj} = 0.026$, denovolyzeR model; Bonferroni correction).

Discussion

We have applied WES to an ASD cohort with abnormal head circumferences to investigate the efficiency of restricting phenotypes to increase gene discovery and to better resolve ASD genotype–phenotype correlations. Clinically relevant pathogenic and likely pathogenic variants account for 23.9% patients. Specifically, clinically relevant variants account for 19.4% patients with microcephaly or macrocephaly. When we consider the DNMs in candidate genes together, WES diagnostic yields arrive 22.4%. Of note, these genes of which 76.5% clinically relevant pathogenic or likely pathogenic variants are already known to be associated with macrocephaly or microcephaly. In addition, we could miss some potential clinically relevant variants with postzygotic *de novo* mutations since we only consider variants with AB above 0.25 which is not very sensitive for mosaic mutations. These data provide evidence that the phenotype-to-genotype approach is useful to detect variants or genes associated with specific phenotype.

We analyzed the detailed clinical information for patients with clinically relevant pathogenic and likely pathogenic mutations. Our study expanded the phenotype spectrum of several ASD and related NDD genes recently identified, including *RAB11B* and *WDR26*. *RAB11B* missense DNMs are also extremely rare among NDDs. Only five patients with *RAB11B* missense DNMs have been reported[33], and four of them have microcephaly. The phenotype of our patient is consistent with those reported patients, including ID, absent speech, and abnormal MRI. Specifically, recurrent missense DNMs of *RAB11A*, an important homolog of *RAB11B*, were identified in patients with epilepsy and/or DD[35]. *WDR26* was recently identified causing a recognizable NDD syndrome, and more than half of the patients showed autistic behaviors and share microcephaly[34]. *WDR26* involves in Wnt-signaling and PI3K-AKT pathway and directly interacts with *GNB1*, a newly identified NDD gene[36]. The function of *WDR26* as it relates to neurodevelopment remains to be investigated.

Our study also provides further genetic evidence for several ASD candidate risk genes, especially within the Chinese cohort, including *UBN2*, *BIRC6*, *SYNE1* and *KCNMA1*. *UBN2* was recently indicated in ASD risk[19], but the function of this gene is completely unknown. Gene ontology annotations related this gene to DNA binding transcription factor activity. Dozens of *BIRC6* missense DNMs have been reported in patients with NDDs (denovo-db), although *de novo* burden has not yet achieved statistical significance. Homozygous *SYNE1* missense mutations have been reported to cause ASD while homozygous truncated mutations cause cerebellar ataxia[37] and a recessive form of arthrogryposis multiplex congenital[38]. Although no other mutation within this gene was identified in the same patient and the pathogenesis of the missense DNM identified in this study is still uncertain, several *SYNE1* missense DNMs have been reported in NDD patients (denovo-db)[23]. *KCNMA1* encodes the α-subunit of the large conductance Ca^{2+}-activated K^{+} channel (BK channels), which plays an essential role in neuronal excitability. Disruption of *KCNMA1* was reported in a single ASD case[39], and several missense DNMs have been reported (denovo-db). Recently, Liang et al. reported nine patients with *de novo KCNMA1* missense variants and a broad spectrum of neurodevelopmental and neurological phenotypes including autistic features[40].

In addition to the variants within known ASD candidate genes, our results also implicate a novel candidate gene, *TNPO3*. *TNPO3* encodes a nuclear import receptor for serine/arginine-rich (SR) proteins. Unfortunately, the function of this gene in neurodevelopment has not been investigated. Further genetic study and functional assays are needed to investigate the role of this gene in ASD risk and neurodevelopment.

Supplementary Material

Refer to Web version on PubMed Central for supplementary material.

Acknowledgements

We thank Tonia Brown for assistance in editing this manuscript. We are grateful to all of the families at the participating this study. This work was supported by the following grants: the National Natural Science Foundation of China (81330027, 81525007, 81671122, 31400919, 31671114) to K.X., Z.H. and H.G.; the Natural Science Foundation of Hunan Province (2016RS2001, 2016JC2055, 2018SK1030, 2018DK2016) to K.X. and Z.H.; the U.S. National Institutes of Health (NIH) (R01MH10221) to E.E.E. H.G. was also supported by the China Hunan Provincial Science & Technology Department (2019RS2005). E.E.E. is an investigator of the Howard Hughes Medical Institute.

References

1. Lai MC, Lombardo MV, Baron-Cohen S. Autism. Lancet (London, England). 2014;383(9920):896–910.
2. Blazejewski SM, Bennison SA, Smith TH, Toyo-Oka K. Neurodevelopmental Genetic Diseases Associated With Microdeletions and Microduplications of Chromosome 17p13.3. Frontiers in genetics. 2018;9:80. [PubMed: 29628935]
3. de la Torre-Ubieta L, Won H, Stein JL, Geschwind DH. Advancing the understanding of autism disease mechanisms through genetics. Nature medicine. 2016;22(4):345–361.
4. Bernier R, Golzio C, Xiong B, et al. Disruptive CHD8 mutations define a subtype of autism early in development. Cell. 2014;158(2):263–276. [PubMed: 24998929]
5. van Bon BW, Coe BP, Bernier R, et al. Disruptive de novo mutations of DYRK1A lead to a syndromic form of autism and ID. Mol Psychiatry. 2016;21(1):126–132. [PubMed: 25707398]
6. Helsmoortel C, Vulto-van Silfhout AT, Coe BP, et al. A SWI/SNF-related autism syndrome caused by de novo mutations in ADNP. Nature genetics. 2014;46(4):380–384. [PubMed: 24531329]
7. Stessman HA, Bernier R, Eichler EE. A genotype-first approach to defining the subtypes of a complex disease. Cell. 2014;156(5):872–877. [PubMed: 24581488]
8. Kanner L Autistic disturbances of affective contact. Nervous Child. 1943;2:217–250.
9. Liaw D, Marsh DJ, Li J, et al. Germline mutations of the PTEN gene in Cowden disease, an inherited breast and thyroid cancer syndrome. Nature genetics. 1997;16(1):64–67. [PubMed: 9140396]
10. Scala E, Ariani F, Mari F, et al. CDKL5/STK9 is mutated in Rett syndrome variant with infantile spasms. Journal of medical genetics. 2005;42(2):103–107. [PubMed: 15689447]
11. Qureshi AY, Mueller S, Snyder AZ, et al. Opposing brain differences in 16p11.2 deletion and duplication carriers. The Journal of neuroscience : the official journal of the Society for Neuroscience. 2014;34(34):11199–11211. [PubMed: 25143601]
12. Li H, Durbin R. Fast and accurate long-read alignment with Burrows-Wheeler transform. Bioinformatics (Oxford, England). 2010;26(5):589–595.
13. McKenna A, Hanna M, Banks E, et al. The Genome Analysis Toolkit: a MapReduce framework for analyzing next-generation DNA sequencing data. Genome research. 2010;20(9):1297–1303. [PubMed: 20644199]

14. Manichaikul A, Mychaleckyj JC, Rich SS, Daly K, Sale M, Chen WM. Robust relationship inference in genome-wide association studies. Bioinformatics (Oxford, England). 2010;26(22):2867–2873.
15. Turner TN, Coe BP, Dickel DE, et al. Genomic Patterns of De Novo Mutation in Simplex Autism. Cell. 2017;171(3):710–722.e712. [PubMed: 28965761]
16. Wang K, Li M, Hakonarson H. ANNOVAR: functional annotation of genetic variants from high-throughput sequencing data. Nucleic acids research. 2010;38(16):e164. [PubMed: 20601685]
17. Fromer M, Moran JL, Chambert K, et al. Discovery and statistical genotyping of copy-number variation from whole-exome sequencing depth. American journal of human genetics. 2012;91(4):597–607. [PubMed: 23040492]
18. Lelieveld SH, Reijnders MR, Pfundt R, et al. Meta-analysis of 2,104 trios provides support for 10 new genes for intellectual disability. Nature neuroscience. 2016;19(9):1194–1196. [PubMed: 27479843]
19. RK CY, Merico D, Bookman M, et al. Whole genome sequencing resource identifies 18 new candidate genes for autism spectrum disorder. Nature neuroscience. 2017;20(4):602–611. [PubMed: 28263302]
20. De Rubeis S, He X, Goldberg AP, et al. Synaptic, transcriptional and chromatin genes disrupted in autism. Nature. 2014;515(7526):209–215. [PubMed: 25363760]
21. Deciphering Developmental Disorders S Prevalence and architecture of de novo mutations in developmental disorders. Nature. 2017;542(7642):433–438. [PubMed: 28135719]
22. Iossifov I, O'Roak BJ, Sanders SJ, et al. The contribution of de novo coding mutations to autism spectrum disorder. Nature. 2014;515(7526):216–221. [PubMed: 25363768]
23. Turner TN, Yi Q, Krumm N, et al. denovo-db: a compendium of human de novo variants. Nucleic acids research. 2017;45(D1):D804–d811. [PubMed: 27907889]
24. O'Roak BJ, Vives L, Fu W, et al. Multiplex targeted sequencing identifies recurrently mutated genes in autism spectrum disorders. Science (New York, NY). 2012;338(6114):1619–1622.
25. Samocha KE, Robinson EB, Sanders SJ, et al. A framework for the interpretation of de novo mutation in human disease. Nature genetics. 2014;46(9):944–950. [PubMed: 25086666]
26. Retterer K, Scuffins J, Schmidt D, et al. Assessing copy number from exome sequencing and exome array CGH based on CNV spectrum in a large clinical cohort. Genetics in medicine : official journal of the American College of Medical Genetics. 2015;17(8):623–629. [PubMed: 25356966]
27. Kearney HM, Thorland EC, Brown KK, Quintero-Rivera F, South ST. American College of Medical Genetics standards and guidelines for interpretation and reporting of postnatal constitutional copy number variants. Genetics in medicine : official journal of the American College of Medical Genetics. 2011;13(7):680–685. [PubMed: 21681106]
28. Richards S, Aziz N, Bale S, et al. Standards and guidelines for the interpretation of sequence variants: a joint consensus recommendation of the American College of Medical Genetics and Genomics and the Association for Molecular Pathology. Genetics in medicine : official journal of the American College of Medical Genetics. 2015;17(5):405–424. [PubMed: 25741868]
29. Guo H, Duyzend MH, Coe BP, et al. Genome sequencing identifies multiple deleterious variants in autism patients with more severe phenotypes. Genetics in medicine : official journal of the American College of Medical Genetics. 2019;21(7):1611–1620. [PubMed: 30504930]
30. Guo H, Wang T, Wu H, et al. Inherited and multiple de novo mutations in autism/developmental delay risk genes suggest a multifactorial model. Molecular autism. 2018;9:64. [PubMed: 30564305]
31. Moortgat S, Berland S, Aukrust I, et al. HUWE1 variants cause dominant X-linked intellectual disability: a clinical study of 21 patients. European journal of human genetics : EJHG. 2018;26(1):64–74. [PubMed: 29180823]
32. Froyen G, Corbett M, Vandewalle J, et al. Submicroscopic duplications of the hydroxysteroid dehydrogenase HSD17B10 and the E3 ubiquitin ligase HUWE1 are associated with mental retardation. American journal of human genetics. 2008;82(2):432–443. [PubMed: 18252223]

33. Lamers IJC, Reijnders MRF, Venselaar H, et al. Recurrent De Novo Mutations Disturbing the GTP/GDP Binding Pocket of RAB11B Cause Intellectual Disability and a Distinctive Brain Phenotype. American journal of human genetics. 2017;101(5):824–832. [PubMed: 29106825]

34. Skraban CM, Wells CF, Markose P, et al. WDR26 Haploinsufficiency Causes a Recognizable Syndrome of Intellectual Disability, Seizures, Abnormal Gait, and Distinctive Facial Features. American journal of human genetics. 2017;101(1):139–148. [PubMed: 28686853]

35. Hamdan FF, Myers CT, Cossette P, et al. High Rate of Recurrent De Novo Mutations in Developmental and Epileptic Encephalopathies. American journal of human genetics. 2017;101(5):664–685. [PubMed: 29100083]

36. Petrovski S, Kury S, Myers CT, et al. Germline De Novo Mutations in GNB1 Cause Severe Neurodevelopmental Disability, Hypotonia, and Seizures. American journal of human genetics. 2016;98(5):1001–1010. [PubMed: 27108799]

37. Gros-Louis F, Dupre N, Dion P, et al. Mutations in SYNE1 lead to a newly discovered form of autosomal recessive cerebellar ataxia. Nature genetics. 2007;39(1):80–85. [PubMed: 17159980]

38. Attali R, Warwar N, Israel A, et al. Mutation of SYNE-1, encoding an essential component of the nuclear lamina, is responsible for autosomal recessive arthrogryposis. Human molecular genetics. 2009;18(18):3462–3469. [PubMed: 19542096]

39. Laumonnier F, Roger S, Guerin P, et al. Association of a functional deficit of the BKCa channel, a synaptic regulator of neuronal excitability, with autism and mental retardation. The American journal of psychiatry. 2006;163(9):1622–1629. [PubMed: 16946189]

40. Liang L, Li X, Moutton S, et al. De novo loss-of-function KCNMA1 variants are associated with a new multiple malformation syndrome and a broad spectrum of developmental and neurological phenotypes. Human molecular genetics. 2019;28(17):2937–2951. [PubMed: 31152168]

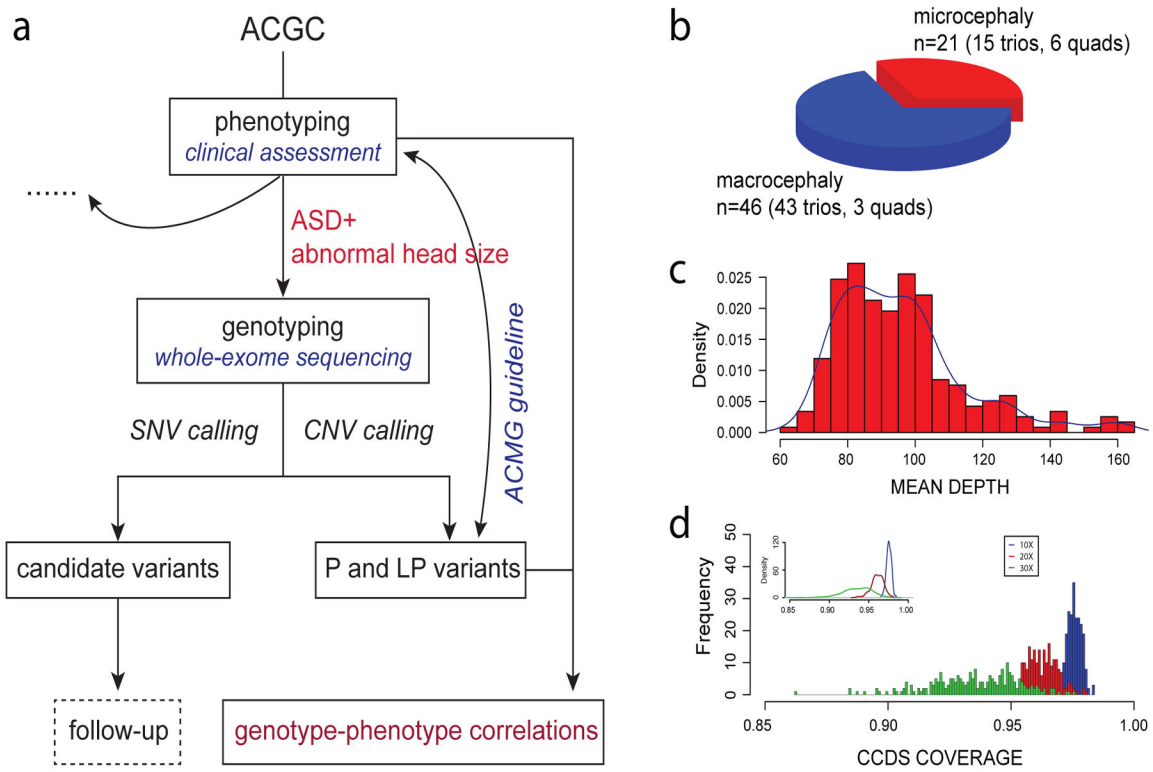

Figure 1.

Schematic of phenotype-to-genotype strategy and the performance of whole-exome sequencing (WES). (a). Schematic of phenotype-to-genotype strategy on the identification of genotype-specific variants or genes in this study. P and LP represent the pathogenic and likely pathogenic variants according to ACMG guidelines. (b) Pie plot shows the number distribution for macrocephaly and microcephaly families involved in this study. (c) Histogram shows the mean depth distribution of WES. (d) Histogram shows the mean coverage distribution of WES.

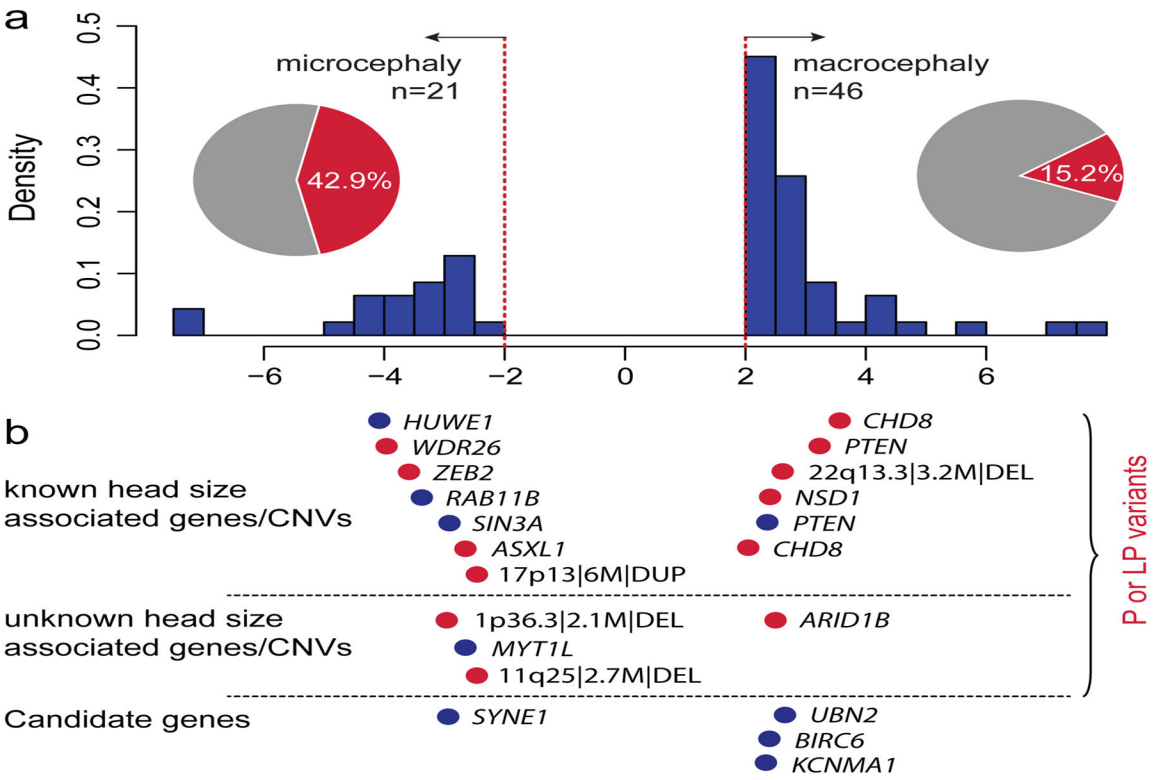

Figure 2.

The relationship between putative disorder-related variants and head circumference. (a) Shown is the distribution of the head circumference standard deviation for the studied samples. The pie plots show the diagnosed yield (only considering pathogenic and likely pathogenic variants) of WES in microcephaly and macrocephaly families. (b) The dot plot shows the head circumference standard deviation of the corresponding clinically relevant and candidate variants. Red dots represent the LGD mutations or CNVs; blue dots represent the missense variants. P and LP represent the pathogenic and likely pathogenic variants according to ACMG guidelines.

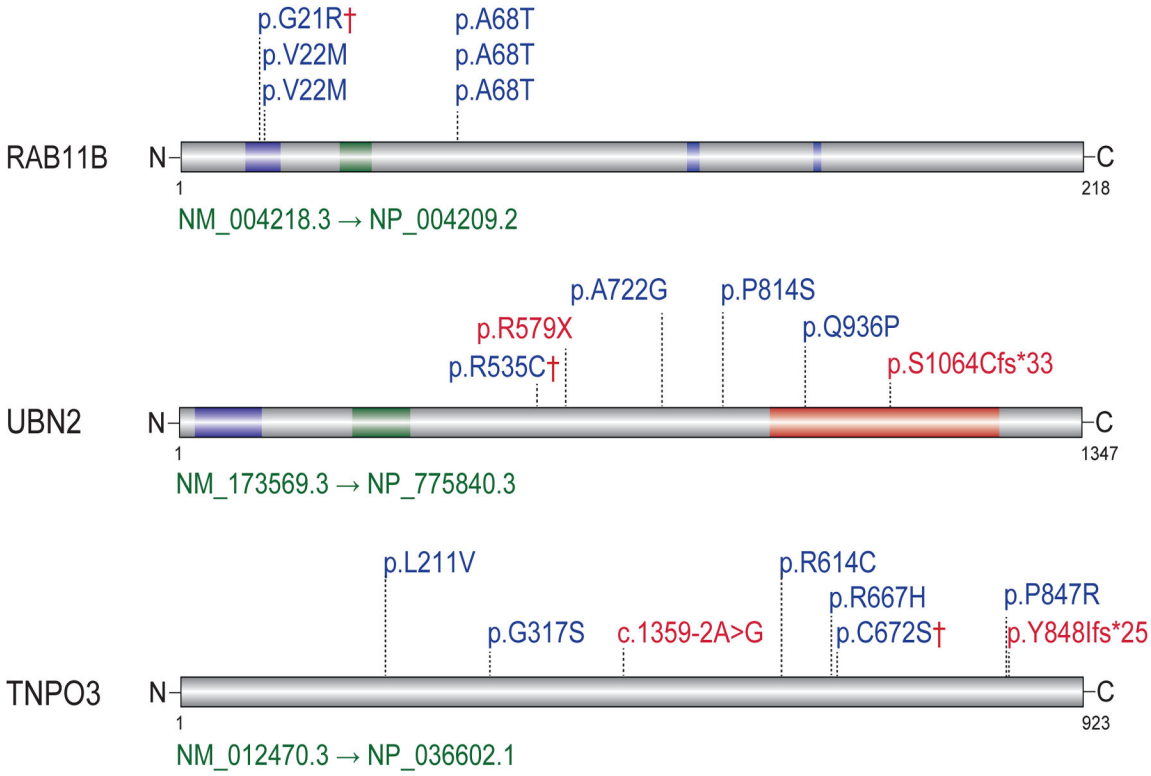

Figure 3.

The Spectrum of *de novo* mutations (DNMs) within one known (*RAB11B*) and two candidate genes (*UBN2*, *TNPO3*). Diagrams of the canonical isoform with DNMs from this study indicated with a dagger (†) and from the published whole-exome or whole-genome sequencing studies of large NDD cohorts are displayed for each gene. Red indicates LGD, and blue indicates missense.

Table 1.

Disorder-related SNVs/indels and head-size association.

Chr	Start(hg38)	End(hg38)	Ref	Alt	Gene	Function[1]	NT&AAchange[2]	CADD	Sample ID	Inheritance	Ma/Mi[3]	HCZ(SD)[4]
Pathogenic variants												
10	87961101	87961101	T	-	*PTEN*	FS	NM_000314:c.1009delT:p.S338Lfs*6	.	GX0427.p1	*de novo*	Ma	+3.23
14	21399998	21399998	T	-	*CHD8*	FS	NM_001170629:c.4800delA:p.G1602Vfs*13	.	HEN0083.p1	*de novo*	Ma	+2.00
14	21408388	21408388	T	-	*CHD8*	FS	NM_001170629:c.2654delA:p.N885Tfs*14	.	GX0540.p1	paternal	Ma	+3.58
5	177191982	177191982	T	A	*NSD1*	SG	NM_022455:c.T1026A:p.C342*	35	HN0038.p1	*de novo*	Ma	+2.38
2	144404880	144404880	-	G	*ZEB2*	FS	NM_014795:c.547_548insG:p.L183Rfs*16	.	GX0430.p1	*de novo*	Mi	−3.55
1	224433889	224433889	T	-	*WDR26*	FS	NM_025160:c.217delA:p.S73Afs*2	.	GX0486.p1	*de novo*	Mi	−3.92
20	32435608	32435611	GGAG	-	*ASXL1*	FS	NM_015338:c.2896_2899del:G966Afs*17	.	GX0468.p1	*de novo*	Mi	−2.54
19	8399883	8399883	G	C	*RAB11B*	MIS	NM_004218:c.G61C:p.G21R	35	GX0152.p1	*de novo*	Mi	−3.31
2	1892087	1892087	C	A	*MYT1L*	SG	NM_001303052:c.G2233T:p.E745*	45	GX0391.p1	*de novo*	-	−2.54
Likely pathogenic variants												
10	87960901	87960901	T	A	*PTEN*	MIS	NM_000314:c.T809A:p.M270K	27.8	HEN0197.p1	*de novo*	Ma	+2.31
15	75371990	75371990	T	C	*SIN3A*	MIS	NM_001145358:c.A3811G:p.K1271E	17.6	GX0044.p1	*de novo*	Mi	−2.77
X	53536461	53536461	G	A	*HUWE1*	MIS	NM_031407:c.C12344T:p.A4115V	25.4	HEN0056.p1	*de novo*	Mi	−4.08
6	157181047	157181047	T	C	*ARID1B*	MIS	NM_017519:c.T3175C:p.W1059R	27.5	HN0092.p1	*de novo*	-	+2.46
Candidate variants												
7	139272328	139272328	C	T	*UBN2*	MIS	NM_173569:c.C1603T:p.R535C	35	HEN0155.p1	*de novo*	-	+2.72
2	32547917	32547917	C	T	*BIRC6*	MIS	NM_016252:c.C12878T:p.T4293I	33	GX0203.p1	*de novo*	-	+2.38
7	128979029	128979029	C	G	*TNPO3*	MIS	NM_012470:exon16:c.G2015C:p.C672S	22.8	GX0226.p1	*de novo*	-	+2.69
6	152211563	152211563	C	T	*SYNE1*	MIS	NM_182961:c.G22520A:p.R7507H	33	HN0048.p1	*de novo*	-	−2.92
10	76891619	76891619	C	T	*KCNMA1*	MIS	NM_001161352:c.G3248A:p.R1083K	22.2	GX0306.p1	*de novo*	-	+2.23

Notes:

1. FS represents frameshift variant, SG represents stop-gain variant, MIS represents missense variants.

2. The canonical isoforms are listed.

3. Ma/Mi represent known macrocephaly (Ma) and microcephaly (Mi) association for the respective genes.

4. HCZ represents head circumference-for-age Z-scores.

Table 2.

Pathogenic CNVs identified in this cohort.

Interval (hg38)	Size	CNV	Sample	Size	Region	GeneNum	ASD gene	Ma/Mi[1]	HCZ (SD)[2]
17:156213–6120665	5.96M	DUP	GX0309.p1	5.96M	17p13.2–13.3	131	*YWHAE*	Micro	−2.31
11:132310051–134986787	2.68M	DEL	GX0309.p1	2.68M	11q25	14	*NTM*	-	−2.31
22:47625313–50799120	3.17M	DEL	HEN0131.p1	3.17M	22q13.3	47	*SHANK3*	Macro	+2.54
1:733013–2789669	2.06M	DEL	GX0418.p1	2.06M	1p36.3	75	*GNB1*	-	−2.85

Notes:

1. Ma represents macrocephaly, Mi represents microcephaly.

2. HCZ represents head circumference-for-age Z-scores.